High Strength Impact Welding of HSLA 340 to Al 5754 and Application Prototype

Yu Mao[1], Brian Thurson[1], Jianxiong Li[1], Anupam Vivek[1]*, Glenn Daehn[1]

[1] Department of Materials Science and Engineering, The Ohio State University, USA
*Corresponding author. Email: vivek.5osu.edu

Abstract

Vaporizing Foil Actuator Welding (VFAW) technique was applied to join 4 mm thick aluminium alloy 5754 to 2.5 mm thick High Strength Low Alloy (HSLA) steel 340 with a 1 mm thick aluminium alloy 3003-H14 interlayer. Welds with consistent peak loads of 17.6 kN were achieved with input energy less than 5 kJ. Tension-tension fatigue testing yielded high cycle around 1000k cycles under the peak load of 40% tensile strength from static testing. Microscopic characterization revealed no continuous melting zones in the welding interfaces. Coupled with lightweight designs, the approach was utilized on prototype production of an aluminium-steel vehicle subframe. Issues related to arcing arose and were tackled during the development of prototype production.

Keywords

Vaporizing foil actuator welding, Impact welding, High Strength Low Alloy steel, Lightweighting, High cycle fatigue, Prototype demonstration

1 Introduction

The road to automotive lightweighting has been explored with more attention than ever during the past decades. Automakers have been pushed rigorously by aggressive policies related to fuel economy and restricted global gas emissions (Meckling and Nahm, 2019). To survive in the market with maintained profits after emerging emission related taxes, automobile giants tackled the challenge with multiple strategies, among which lightweighting by material substitution is considered as a key technology strategy (Kelly et al., 2015). Conventionally, car bodies are made of steel, as it is the most preferable

material in the automotive industry with decent mechanical properties, and most importantly, low cost (Singh, 2016). However, given that the weight-driven emission expense is now adding on to the capitalized cost, lightweight materials with high strength-to-weight ratios such as high-strength steel, aluminium alloys, magnesium alloys, carbon fiber, etc. are increasingly applied in the automotive world coupled with lightweight designs (Taub and Luo, 2015). However, conventional joining technologies, mostly designed for traditional steel materials, are not as capable or mostly impossible for the new materials. Fusion-based welding, e.g., resistance spot welding, metal inert gas welding (MIG) and tungsten inert gas welding (TIG) are the benchmark welding technologies in automobile industry, but they are limited by formation of heat affected zones (HAZ) and brittle intermetallic compounds (IMC) for dissimilar joint due to disparities between melting points of the materials, which dramatically downgrades the properties of the joint (Lee et al., 2000). Non-metallic bonding methods, such as mechanical fasteners and adhesive bonding are currently widely used for dissimilar joining (Barnes and Pashby, 2000), but concerns on additional labor cost, poor fatigue properties due to stress concentration for fasteners, and limitation in shear strength and high-temperature performance for adhesives restrain their development to next level in vehicles (Meschut et al., 2014; Mori et al., 2006; Sankaranarayanan and Hynes, 2018). Advanced welding techniques, represented by solid-state welding including friction-stir welding (FSW), and diffusion bonding can minimize large scale melting and create the solid state joining at temperatures below the melting points. However, a heating process is still involved, FSW normally occurs at the temperature of 0.6~0.8*Tm where Tm is the melting point of the metal (Dadi et al., 2020). This therefore creates HAZ and IMC as well as thermo-mechanically affected zones (TMAZ) for FSW (Bussu and Irving, 2002). Ultrasonic welding method can minimize the HAZ and TMAZ formation but it is limited to thin parts (Tilahun et al., 2020).

Impact welding methods can minimize the HAZ, TMAZ and IMC formation observed in traditional methods and are very versatile in dissimilar metal joining (Vivek et al., 2013). Vaporizing foil actuator welding (VFAW), an impact welding process, has shown great potential to join various dissimilar lightweight metals such as Al/high-strength steel (Kapil et al., 2020), Al/Mg (Vivek et al., 2013), Al/Ti (Chen et al., 2019) with preservation of the strength of base metals. The technique achieves welds of preferable geometries and configurations for multi-material lightweight designs in automobile manufacturing. As a solid-state welding approach, VFAW forms little to no HAZ or IMCs in the welding interface, the strength of the parent metals can therefore be retained.

Here we show a novel approach of VFAW to create high strength solid state welds between thick Al 5754 and HSLA 340 and its application on vehicle engine cradle prototype. Microstructural characterization, lap shear testing, and fatigue testing were performed to examine the samples and validate the welding process. During prototype production, arcing issues which were deleterious to the process occurred. Modifications on tooling was designed and tested and solved the issue.

2 Approach

4 mm thick AA 5754 sheet was used as the flyer. 2.5 mm thick HSLA 340 sheet was selected as the target. A 1 mm thick Al 3003-H14 was selected as the interlayer. Both of the Al 3003 interlayer sheet and HSLA 340 target sheet were preformed to create space for acceleration and impact. A third material is widely used as an interlayer in EXW to join metals with a high yield strength, a high strain hardening exponent, or a high-quality bonded interface (Manikandan et al., 2008). The interlayer is normally a weaker metal with better weldability. The function of the interlayer is to reduce the kinetic energy dissipation of the flyer, increase the heat transfer area (Saravanan and Raghukandan, 2013), and therefore decrease the formation of the IMCs (Han et al., 2003). Manikandan et al. compared the EXWed titanium/304 stainless steel with and without an interlayer and proved the involvement of the interlayer reduced the kinetic energy loss which would have resulted in molten zones at the interface; instead, this part of energy causes the formation of the IMC-free wavy interface at the interlayer (Manikandan et al., 2008). Saravanan and Raghukandan proposed that the involvement of the interlayer significantly lowered the boundary of the weldability window of the two initial materials (Saravanan and Raghukandan, 2013). In this work, 3000 series aluminium alloy is selected as the interlayer material for VFAW aluminium alloys to steel because of 1) its similar nature to high-strength aluminium, 2) the highest liquidous temperature among aluminium alloys, and 3) a relatively low strength. Various work on explosive welding for Al-steel clads had an Al 3003 involved and showed a positive effect on welding strength (Carvalho et al., 2019; Izuma et al., 1992).

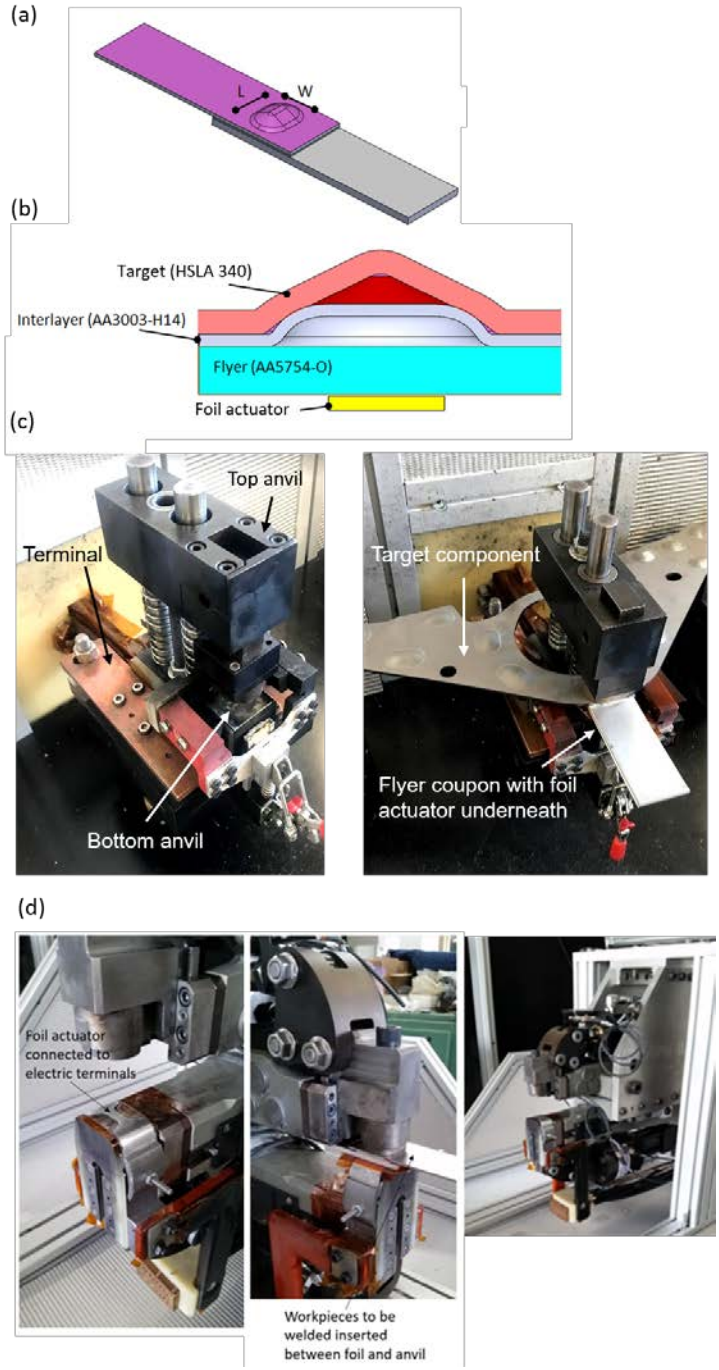

Figure 1*: Illustration of VFAW with interlayer: (a) L and W are length and width of the dimples; (b) the cross-section view of the experiment setup.*

The designed weld has a pellet shape with a size of 20 mm wide by 30 mm long, depicted in Fig. 1a. To achieve welds with smaller size is a goal for flange configuration, which is widely used in structural components in vehicles. A 0.0762 mm thick aluminium foil actuator was used. Parallel and perpendicular configurations between the foil and longitude of the weld was tested respectively. The energy source is a capacitor bank system with max charging energy of 4.2 kJ, capacitance of 50 μF, and short-circuit current rise time of 6 μs.

The welding setup is shown in Fig. 1b. During welding, the aluminium actuator is rapidly vaporized into high pressure plasma, driving the AA5754 flyer into the space created by the pre-deformed interlayer and the first impact occurs between the flyer and the interlayer, followed by the second impact between the interlayer and the target. Fig. 1c shows the welding tool that was used to make the welds on which the mechanical test data is reported while the tool shown in Fig. 1d is a robot-mountable welding head that was used for welding the prototype component. Optical microscopic characterization was performed to investigate the microstructure of the welding interface. Lap shear testing with a strain rate of 0.1 mm/s was employed. Based on the average of the static failure load from the lap shear testing, fatigue test with peak loads ranging from 40% to 60% of tensile strength were performed with 10 Hz tension-tension mode.

3 Results and Discussion

3.1 Mechanical testing

Fig. 2a shows a typical AA 5754/HSLA 340 impact weld. The results of lap shear testing are shown in Fig. 2b. The welds exhibit an average peak load of 17.6 kN with great consistency. The failure occurred at the interface between the AA 3003 interlayer and HSLA 340 target, where a clear material transfer of AA 3003 was observed. It indicates the failure was in the mode of shearing of the AA 3003 interlayer. The two weld-foil configurations created welds with identical strength, which enables the flexibility during the production process.

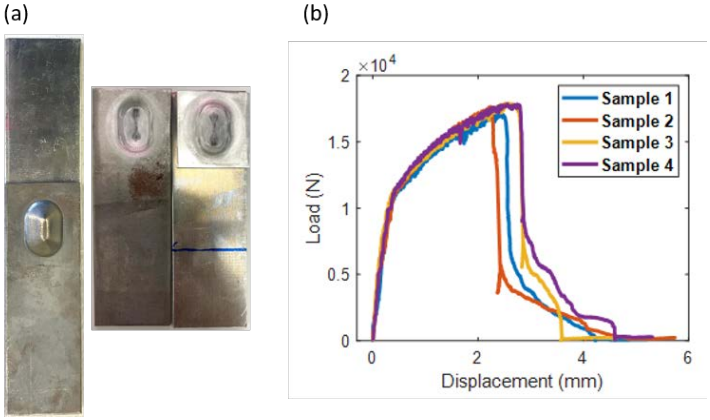

***Figure 2**: VFA welded AA5754-HSLA340: (a) as welded and after lap shear testing and (b) load-displacement curves during lap shear testing.*

The results of the fatigue test are shown in Fig. 3 with the samples failed with different failure modes. The results show that high cycle around 1000k cycles was achieved under the peak load of 40% tensile strength and a failure at AA 5754 base metal was yielded, which is caused by cracking propagation on the AA 5754 flyer. Fatigue data on peak loads of 50% and 60% tensile strength shows acceptable repeatability on failure cycles around

80k and 20k, resulting in an interfacial failure between the interlayer and target, which is identical to the failure mode of static tests.

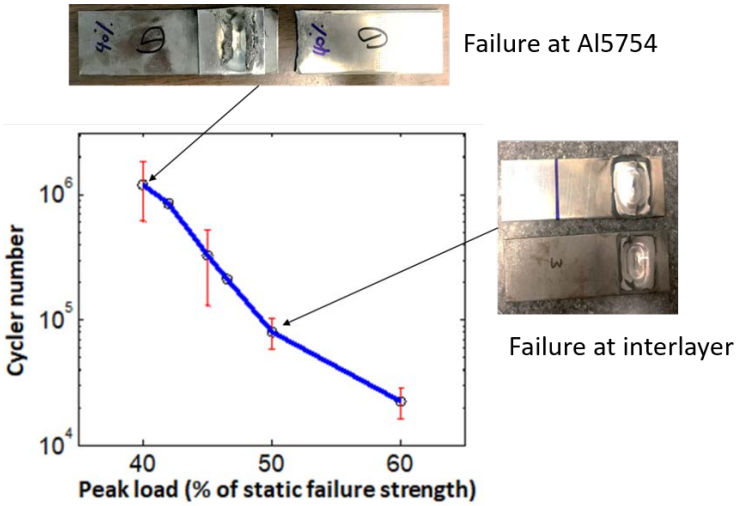

***Figure 3**: Cycles to failure versus peak loads in fatigue tests of VFA welds of Al 5754-HSLA 340 and the representative failure modes at high and low cycle tests.*

3.2 Microstructure

Fig. 4 shows the cross-sectional microstructures for AA5754/HSLA340 impact welds. Four typical types of joining interface between the Al 3003 interlayer and HSLA 340 target were observed. These are unwelded area, welded area with no intermetallic compounds (IMC), welded area with discontinuous IMC, and area with locally continuous IMC. The heterogeneous microstructures were formed due to the variation of impact angle and velocity in the VFAW process (Li et al., 2020). Localized melting and solidification, the reason for the IMC formation, is not an uncommon phenomenon in impact welding. This is caused by the trapped dissipative heating during the impact welding process. The distributions of the IMC along the interface have a significant influence on the mechanical properties. The continuous IMC between iron and aluminium is brittle and therefore easily cracked under low stress (Fig. 4a). Therefore, reducing the formation of continuous IMC can be critical. A perfect interface is IMC free, but a joining interface with discontinuous IMC in pockets is also acceptable because the crack will be arrested by the IMC free zones. The waviness is small in this weld as it is proved that the waviness is not necessary for a strong weld (Szecket et al., 1985). Among the four typical areas, the IMC free area and area with discontinuous IMC are considered effective welded area between interlayer and HSLA 340 target which provide the high mechanical strengths observed in Figs. 2 and 3. Similar microstructure was observed by Kapil et al. in the impact welding of Aural 2 to HSLA 340 HDGI (Kapil et al., 2020).

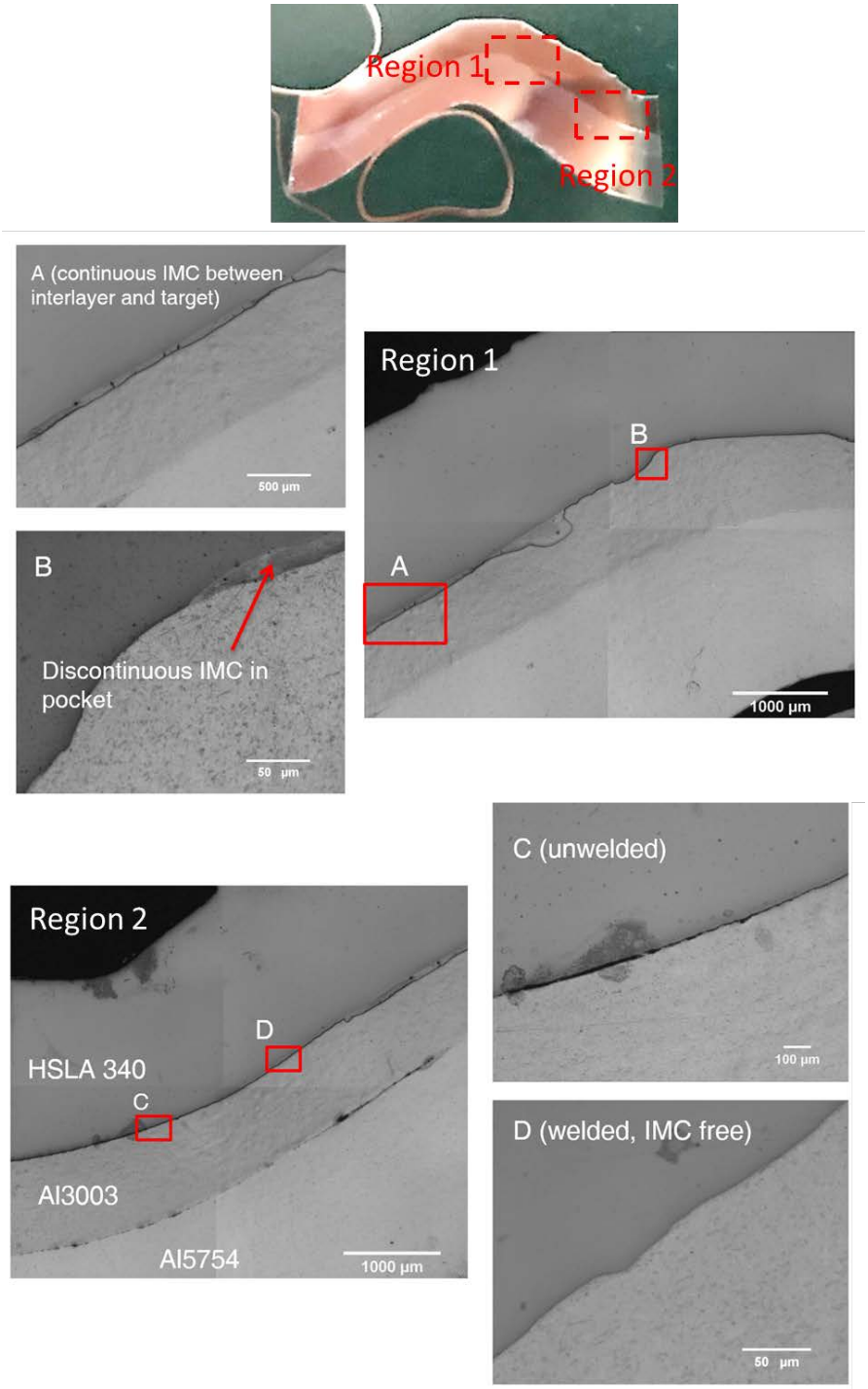

***Figure 4**: Microscopic cross-section images of the welding interface of Al 5754-HSLA 340. Four typical regions in AA3003/HSLA 340 interface were categorized: locally continuous IMC zone (A), discontinuous IMC zone (B), unwelded zone (C), and IMC-free welded zone (D)*

3.3 Prototype production and arcing issue

With the proposed VFAW approach, prototype production was achieved on the multi-material subframes consisting of parts of 4.5 mm thick AA 5182 and 2.5 mm thick HSLA 340 (Fig. 5). To achieve better energy efficiency and maximum robustness, the interlayer was firstly welded to the preformed target and then the AA 5182 part was welded to the HSLA 340 target at the interlayer.

Figure 5*: Two VFA welded prototype subframes (in progress).*

Arcing issues were detected, analysed, and solved. Three locations where arcing mostly occurred, shown in Fig. 6, were redesigned: (1) the terminal connection to co-axial cable and it was solved by redesign of the connection part, shown in Figure 6a. (2) The hot bus bar area where there are lots of close edges of the bar and anvil, and it was solved by creating extra space in-between and separating them with an extra G10 piece, shown in Figure 6b. (3) The fasteners of the terminals on welding head where the two thru holes caused arcing from hot copper terminal to the anvil and copper bar to the metal screw, and it was solved by adding space with rubber O-rings, thicker G10 sheets and Teflon blocks, shown in Figure 6c. The system was proved robust and functional for VFA welding after the upgrade.

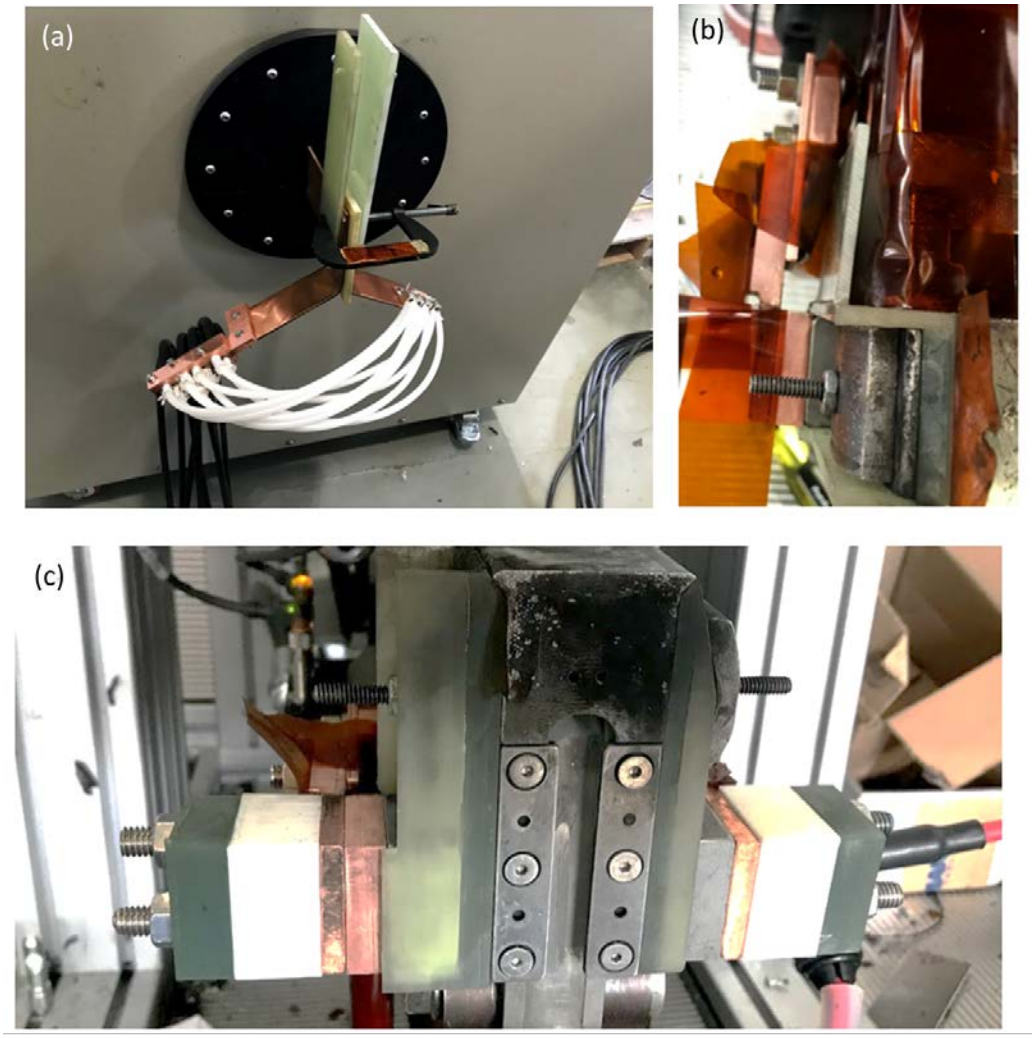

***Figure 6**: Regions of arcing issue and redesign solutions*

Ideally, when a capacitor bank is discharged for a VFA weld the electrical energy will only travel through the buss work and the foil on its path to the ground side of the capacitor bank. In practice the electric current can find paths to ground that deviate from the path through the foil. These deviations in the electrical circuit typically take the form of electrical arcs. These arcs can cause severe damage to ancillary equipment and can pose a safety hazard if the electrical energy can find paths to the ground side of the capacitor bank which are not intended. For example, if an arc jumps to the body of a welding fixture which is connected to ground through a piece of equipment (robot, hydraulic unit, diagnostic equipment etc.) then all or a portion of the electrical discharge of the capacitor will travel through that equipment and into the electrical socket powering the equipment. Once the energy reaches the electrical socket it will travel through the wiring of the building until it reaches the electrical plug for the capacitor bank. This phenomenon is referred to as a ‘ground loop’ and is to be avoided for human and equipment safety.

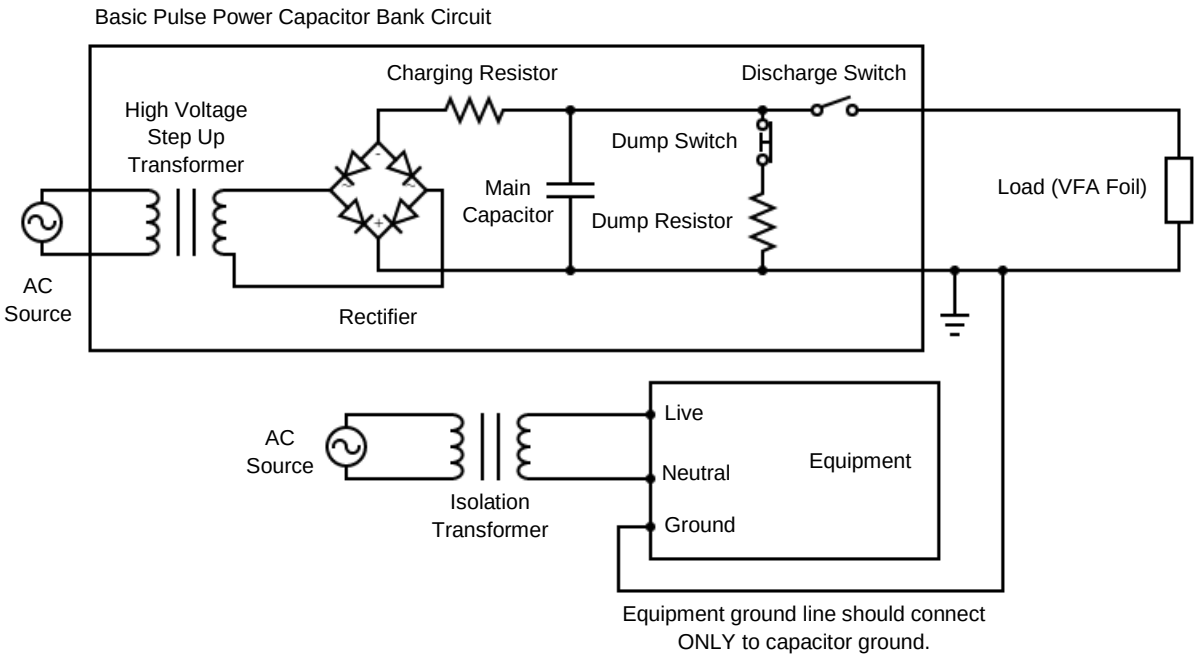

***Figure 7**: General schematic of ancillary equipment integration with a pulsed power system.*

Figure 7 gives guidance on how to correctly wire equipment which may be exposed to electrical arcs, or which is electrically connected to any conductors which may be exposed to arcs. It should be noted that the equipment is powered through an isolation transformer and is grounded not through a wall socket but instead to the capacitor bank's ground buss bar (which is typically connected directly to earth ground). The isolation transformer breaks direct electrical connections to the live and neutral wires of a building's electrical system. Neutral wires are typically connected to ground in the building's junction box, if not for the isolation transformer a ground loop passing through the equipment would be possible. Proper grounding of the capacitor bank and ancillary equipment will protect workers and unrelated equipment powered through the building's electrical system. Electrical arcs may still induce damaging currents in the equipment if the arcs travel through the equipment to ground. Equipment should be kept away (10cm or more) from the buss work, the vaporizing foil, and any large or awkwardly shaped workpieces (power can travel through workpieces to nearby equipment). If equipment does not need to be electrically connected to the capacitor bank and if the equipment can be kept far enough away such that arcing is impossible then the equipment can be wired normally. Equipment should be kept physically and electrically isolated from the capacitor bank whenever possible.

An understanding of typical electrical wiring is necessary when setting up capacitor banks. It should be noted that the ground and neutral wires are electrically connected at the building's junction box. Isolation transformers typically come with a ground wire which passes through to the output side and which connects to the metal body of the transformer, this will need to be disconnected. Any equipment powered through an isolation transformer should be grounded only to the capacitor bank. Buss bar of the capacitor bank

connected to ground should be identified. The body of the capacitor bank should be connected directly to the grounded buss bar. Test equipment for potentially unexpected ground paths. For example, hydraulic hoses typically will have conductive elements inside and can provide an unexpected ground loop. It should be ensured that workpieces do not contact conductors which cannot tolerate high voltage/current electrical arcs. A simple test for ground loops is to unplug the capacitor bank from the wall and to then test for electrical continuity to ground. If no ground paths exist when the capacitor bank is unplugged, then there should be no ground loops.

4 Conclusion

VFAW has been demonstrated to create high strength welds of AA 5754/HSLA340 with an Al 3003-H14 interlayer. The joints showed remarkable static and dynamic mechanical properties. Heterogeneous microstructures were found in the produced impact welds. The approach was successfully prototyped on automotive subframes. Preventing arcing with adequate insulation between terminals is essential for the VFAW process. Correct grounding on the capacitor bank system is critical for safe and robust operation of the system.

5 Acknowledgements

This work was funded by the U.S. Department of Energy (DOE) Award No. DE-EE0007813. Authors are thankful for collaboration with Coldwater Machine Company, Magna International for design and build of welding tools as well as the prototype components.

References

Barnes, T.A., Pashby, I.R., 2000. Joining techniques for aluminium spaceframes used in automobiles: Part II — adhesive bonding and mechanical fasteners. J. Mater. Process. Technol. 99, 72–79. https://doi.org/10.1016/S0924-0136(99)00361-1

Bussu, G., Irving, P.E., 2002. The role of residual stress and heat affected zone properties on fatigue crack propagation in friction stir welded 2024-T351 aluminium joints. Int. J. Fatigue 25, 77–88. https://doi.org/10.1016/S0142-1123(02)00038-5

Carvalho, G.H.S.F.L., Galvão, I., Mendes, R., Leal, R.M., Loureiro, A., 2019. Microstructure and mechanical behaviour of aluminium-carbon steel and aluminium-stainless steel clads produced with an aluminium interlayer. Mater. Charact. 155, 109819. https://doi.org/10.1016/j.matchar.2019.109819

Chen, S., Huo, X., Guo, C., Wei, X., Huang, J., Yang, J., Lin, S., 2019. Interfacial characteristics of Ti/Al joint by vaporizing foil actuator welding. J. Mater. Process. Technol. 263, 73–81. https://doi.org/10.1016/j.jmatprotec.2018.08.004

Dadi, S.S.O., Patel, C., Appala Naidu, B., 2020. Effect of friction-stir welding parameters on the welding temperature. Mater. Today Proc. 38, 3358–3364. https://doi.org/10.1016/j.matpr.2020.10.364

Han, J.H., Ahn, J.P., Shin, M.C., 2003. Effect of interlayer thickness on shear deformation behavior of AA5083 aluminum alloy/SS41 steel plates manufactured by explosive welding. J. Mater. Sci. 38, 13–18. https://doi.org/10.1023/A:1021197328946

Izuma, T., Hokamoto, K., Fujita, M., Aoyagi, M., 1992. Single-shot explosive welding of hard-to-weld a5083/sus304 clad using sus304 intermediate plate. Weld. Int. 6, 941–946. https://doi.org/10.1080/09507119209548320

Kapil, A., Mao, Y., Vivek, A., Cooper, R., Hetrick, E., Daehn, G., 2020. A new approach for dissimilar aluminum-steel impact spot welding using vaporizing foil actuators. J. Manuf. Process. 58, 279–288. https://doi.org/10.1016/j.jmapro.2020.08.015

Kelly, J.C., Sullivan, J.L., Burnham, A., Elgowainy, A., 2015. Impacts of Vehicle Weight Reduction via Material Substitution on Life-Cycle Greenhouse Gas Emissions. Environ. Sci. Technol. 49, 12535–12542. https://doi.org/10.1021/acs.est.5b03192

Lee, C.S., Chandel, R.S., Seow, H.P., 2000. Effect of welding parameters on the size of heat affected zone of submerged arc welding. Mater. Manuf. Process. 15, 649–666. https://doi.org/10.1080/10426910008913011

Li, J., Schneiderman, B., Gilbert, S.M., Vivek, A., Yu, Z., Daehn, G., 2020. Process characteristics and interfacial microstructure in spot impact welding of titanium to stainless steel. J. Manuf. Process. 50, 421–429. https://doi.org/10.1016/j.jmapro.2019.12.036

Manikandan, P., Hokamoto, K., Fujita, M., Raghukandan, K., Tomoshige, R., 2008. Control of energetic conditions by employing interlayer of different thickness for explosive welding of titanium/304 stainless steel. J. Mater. Process. Technol. 195, 232–240. https://doi.org/10.1016/j.jmatprotec.2007.05.002

Meckling, J., Nahm, J., 2019. The politics of technology bans: Industrial policy competition and green goals for the auto industry. Energy Policy 126, 470–479. https://doi.org/10.1016/j.enpol.2018.11.031

Meschut, G., Janzen, V., Olfermann, T., 2014. Innovative and highly productive joining technologies for multi-material lightweight car body structures. J. Mater. Eng. Perform. 23, 1515–1523. https://doi.org/10.1007/s11665-014-0962-3

Mori, K., Kato, T., Abe, Y., Ravshanbek, Y., 2006. Plastic joining of ultra high strength steel and aluminium alloy sheets by self piercing rivet. CIRP Ann. - Manuf. Technol. 55, 283–286. https://doi.org/10.1016/S0007-8506(07)60417-X

Sankaranarayanan, R., Hynes, N.R.J., 2018. Prospects of joining multi-material structures. AIP Conf. Proc. 1953, 1–5. https://doi.org/10.1063/1.5033165

Saravanan, S., Raghukandan, K., 2013. Influence of interlayer in explosive cladding of dissimilar metals. Mater. Manuf. Process. 28, 589–594. https://doi.org/10.1080/10426914.2012.736665

Singh, M.K., 2016. Application of Steel in Automotive Industry. Int. J. Emerg. Technol. Adv. Eng.

6, 246–253.

Szecket, A., Inal, O.T., Vigueras, D.J., Rocco, J., 1985. A wavy versus straight interface in the explosive welding of aluminum to steel. J. Vac. Sci. Technol. A Vacuum, Surfaces, Film. 3, 2588–2593.

Taub, A.I., Luo, A.A., 2015. Advanced lightweight materials and manufacturing processes for automotive applications. MRS Bull. 40, 1045–1053. https://doi.org/10.1557/mrs.2015.268

Tilahun, S., Vijayakumar, M.D., Ramesh Kannan, C., Manivannan, S., Vairamuthu, J., Manoj Kumar, K.P., 2020. A Review on Ultrasonic Welding of Various Materials and Their Mechanical Properties. IOP Conf. Ser. Mater. Sci. Eng. 988. https://doi.org/10.1088/1757-899X/988/1/012113

Vivek, A., Hansen, S.R., Liu, B.C., Daehn, G.S., 2013. Vaporizing foil actuator: A tool for collision welding. J. Mater. Process. Technol. 213, 2304–2311. https://doi.org/10.1016/j.jmatprotec.2013.07.006